Relation Between High Pressure Blocking and Aerosol Concentrations in Southern Sweden

Fredrik Bergelv

Acknowledgments

Thank you...

Abstract

Abstract...

Contents

1   Introduction

It is common knowledge that Earth's increasing temperature has many side effects. One such effect is the increase in frequency of extreme weather phenomena [2]. One such phenomenon, which lacks extensive research, is high-pressure blocking events. High-pressure blocking events is an anticyclone that covers an area for a prolonged period of time and often blocks other types of weather, hence the name. This results in clearer weather and more extreme temperatures [3]. However, an anticyclone is also associated with lower air movement and wind, causing the air to remain stagnant. This can lead to an accumulation of aerosols such as $PM_{2.5}$ in the region [4].

To investigate the relationship between $PM_{2.5}$ and high-pressure blocking, one must analyse periods of high-pressure blocking and examine the concentration of $PM_{2.5}$ during these periods. The goal of this thesis is to analyse the concentration of $PM_{2.5}$ during periods of high-pressure blocking by examining data from the Swedish Meteorological and Hydrological Institute (SMHI) and $PM_{2.5}$ data from rural (Vavihill, Svalöv Skåne county) and urban (Malmö, Skåne county) areas.

2   Theory

2.1   The physics behind anticyclones

Anticyclones are meteorological high-pressure systems in which air sinks toward the ground, creating high pressure [5]. This occurs due to the convergence of air from all directions, which forces the air to move downward. The descending air undergoes adiabatic compression, resulting in an increase in the energy of air molecules, or, in other words, a higher temperature. This rise in energy inhibits cloud formation, as the air molecules are unable to ascend due to the lack of cooling. The absence of clouds allows solar radiation to significantly impact the temperature during an anticyclone. Consequently, this leads to a large temperature difference between day and night, with summer anticyclones associated with high temperatures and winter anticyclones with low temperatures. Due to the Coriolis effect, anticyclones rotate in a clockwise direction in the Northern Hemisphere.

more on anticyclones

A high-pressure blocking period refers to a prolonged anticyclone characterized by higher surface pressure covering a large area [3]. Since the blocking system extends over a vast region, the pressure gradient remains small due to minimal fluctuations. As a result, winds tend to be calm to gentle breezes. A blocking period is typically defined as lasting between five and ten days, although no single definition exists. While the concept has been recognized in meteorology for over a century, the long-term consequences of blocking events are not yet fully understood. High-

pressure blocking periods are more common in the Northern Hemisphere compared to the Southern Hemisphere. Research has indicated that the frequency of blocking periods has increased in recent years [3].

Recurring anticyclones can be classified into Hess and Brezowsky (1977) macrocirculation types, such as the Fennoscandian High (Hfa), the Southeast Anticyclone (Sea), and the Central European High (HM) [6]. These anticyclones are located at specific geographic points. Since anticyclones exhibit winds rotating clockwise around their center, the winds from (Hfa), (Sea), and (HM) tend to blow toward southern Sweden from the south and east. The transport of airborne pollutants, such as ozone, can occur via these winds [7]. Consequently, it can be hypothesized that other airborne aerosols, such as $PM_{2.5}$, should also be transported through these wind patterns.

Moving anticyclones

2.2   The physics behind PM 2.5

$PM_{2.5}$ refers to particulate matter with a diameter of $2.5\,\mu m$ or less. Although these aerosols can form naturally in the atmosphere, their primary sources include solid fuel combustion for domestic heating, industrial activities, and road transportation [8]. A significant contributor to $PM_{2.5}$ pollution is the bonding of aerosols to ammonia emitted from agricultural activities. The European Union has set an annual mean limit for $PM_{2.5}$ concentrations at $25\,\mu g\,m^{-3}$. This threshold has been exceeded in several countries, including Croatia, Bosnia and Herzegovina, Italy, Poland, North Macedonia, and Türkiye [8]. Studies have demonstrated a correlation between elevated $PM_{2.5}$ concentrations and an increased risk of respiratory, cardiovascular, and cerebrovascular diseases, as well as diabetes.

Since $PM_{2.5}$ emissions are particularly high in countries such as Poland, anticyclonic winds from (Hfa), (Sea), and (HM) are expected to increase $PM_{2.5}$ concentrations in southern Sweden [8]. These aerosols would be transported to southern Sweden via southerly to easterly winds during the anticyclone. If this occurs during a high-pressure blocking event, the aerosols may accumulate over the region while continuously being advected by southerly and easterly winds. Studies in China have shown that the dispersion of aerosols during high-pressure blocking is inhibited [4]. Whether the same occurs in southern Sweden is of interest for further study.

3 Method

3.1 The data handling

The relevant data was downloaded from the SMHI's website as CSV files. These files included hourly atmospheric pressure data, hourly rain data, and hourly wind data (speed and direction). Hourly $PM_{2.5}$ data, measured over one-hour intervals, was also downloaded. Since the goal of this project was to analyse $PM_{2.5}$ concentrations in Southern Sweden during high-pressure blocking events, one urban and one rural site were selected. The locations were chosen based on their classification as rural or urban and the length of time the stations had been in operation, where more data was considered better.

The rural measuring station with the most data was Vavihill (Svalöv, Skåne County, Sweden). This station was active from September 28, 1999, to November 15, 2017. However, due to missing data on some days, only 57 % of the period contained non-NaN values. Additionally, between 2017 and 2018, the Vavihill station was relocated to nearby Hallahus, where it operated from May 10, 2018, to December 31, 2022, with 93 % of the period containing non-NaN values. Combining these datasets resulted in a total of 5,371 days of hourly data. For an urban location in Southern Sweden, Malmö Rådhuset had the most data, with measurements recorded from June 3, 1999, to December 31, 2023. Here, 90 % of the recorded values were non-NaN, resulting in 8,074 days of data.

The choice of atmospheric pressure measurement station was Helsingborg, located 25 km from Vavihill and 49 km from Malmö. This location was chosen based on its proximity to both $PM_{2.5}$ measuring stations, the fact that neither Malmö nor Vavihill have pressure measurements from this period, and the fact that the station has been in use from August 2, 1995, to October 10, 2024, with measurements taken every hour without any missing (NaN) values. This station thus covers the entire period of the $PM_{2.5}$ data. It is important to note that the measurements were shown as sea-level pressure.

The relevant rain and wind data were gathered from two different stations. For Vavihill, the station at Hörby, located 35 km away, was used, and for Malmö, a weather station just 6 km away was used. The weather station at Hörby was chosen instead of Helsingborg since neither Vavihill nor Hörby are located along the coast, whereas Helsingborg is. The wind and rain data from Hörby were measured from August 1, 1995, to October 1, 2020, with measurements taken every hour without any missing (NaN) values. It is important to note that the Hörby station was temporarily relocated for a short period in 2021. The rain data from Malmö was measured from November 21, 1995, and the wind data from January 1, 1990, with both measurements ending on December 31, 2020. These stations did not lack any data.

The las task was to evaluate if high-pressure blocking events had become increasingly more common. For this evaluation, atmospheric pressure data from Ängelholm was used instead of Helsingborg due to the pressure data

from Ängelholm being active from January 5, 1946, to October 1, 2024, meaning it has been in service for 49 years longer than that from Helsingborg. This station is located 44 km from Vavihill and 76 km from Malmö. However, the pressure values differed only by a mean of 0.25 hPa and a standard deviation of 0.20 hPa. The rain data was also expanded by using daily rain data from Ängelholm since this data was gathered from January 18, 1947, to November 30, 2001. To obtain the maximum amount of the the rain data the data from Ängelholm was used together with the nearby station of Tånga. This station is located 12 km away and had been in use between December 19, 1973, to August 31, 2024.

3.2   How the high-pressure blocking evens were found

To evaluate when there was a high-pressure blocking event for Vavihill or Malmö, the rain data and atmospheric air pressure were used. For a period to be defined as a high-pressure event, the atmospheric pressure had to be over 1014 hPa, and the rainfall had to be less than $0.5 \, \mathrm{mm \, h^{-1}}$. These values were based on the fact that 1014 hPa was the mean atmospheric pressure from Helsingborg, and $0.5 \, \mathrm{mm \, h^{-1}}$ was chosen since this is considered light rain. The rain-limit was set to $2 \, \mathrm{mm \, d^{-1}}$ in the case where daily precipitation was used instead. This value was chosen since it corresponds to a small amount of rainfall for a day. The reason for not using a rain-limit corresponding to $0.5 \, \mathrm{mm \, h^{-1}}$ comes down to the fact that constant levels of precipitation at this rate for 24 hours are extremely rare. For a high-pressure event to be considered a high-pressure blocking event, the criteria for a high-pressure event had to persist for at least 120 h (5 days). This value was chosen since a 5-day limit is often considered when classifying high-pressure blocking events.

3.3   The data analysis

The data was analysed by taking the mean and standard deviation of each hour of the high-pressure blocking event, from hour one, to evaluate the average progression of a blocking over time using the Python packages `NumPy` and `pandas`. Since the blocking events varied in length, the number of data points was also plotted, with the requirement that each hour consist of at least 8 data points. This resulted in a plot of the mean concentration of $PM_{2.5}$ for every hour from the beginning of the blocking period, for both Vavihill and Malmö. All of the $PM_{2.5}$ plots were evaluated together with the mean value when there was no blocking and the EU annual mean limit for $PM_{2.5}$. Due to the lack of $PM_{2.5}$ data during some periods, a filter was applied, stating that a period needed 95 % $PM_{2.5}$ coverage in order to be analysed.

Afterwards, the data was sorted in different ways to explore how the $PM_{2.5}$ concentration depended on different parameters. Firstly, the data was sorted into one of four wind categories: North-East (310° to 70°), South-East (70° to 190°), West (190° to 310°), and no specific direction. This was done by categorizing the data if 60 % of the wind directional data fell into one of these categories, with no wind being handled as a NaN value.

Secondly, the data was sorted based on the season of the blocking. This was evaluated by taking the midpoint date of the blocking and categorizing the season by the month it occupied. December, January, and February were considered winter; June, July, and August were considered summer; and spring and autumn were the remaining months. Lastly, the data was categorized based on the strength of the high-pressure blocking, where a weak high-pressure blocking event had a mean atmospheric pressure between 1014 hPa and 1020 hPa, a medium-strength blocking event had a mean atmospheric pressure between 1020 hPa and 1025 hPa, and a strong blocking event had a mean atmospheric pressure over 1025 hPa.

The last task was to evaluate whether high-pressure blocking events had become increasingly more common. This was evaluated in two different ways: by calculating the number of high-pressure blocking events per year, and the number and lengths of high-pressure blocking events per year. The number of days of blocking was also sorted by the season of the blocking to provide more insight into the nature of the high-pressure blocking events.

3.4   Statistical evaluation and the Mann-Kendall test

To evaluate if the plots produced significant results, two tests were performed. The first test compared the mean and standard deviation of $PM_{2.5}$ during high-pressure blocking events with the mean and standard deviation during periods without high-pressure blocking. Secondly, the Mann-Kendall test was performed to evaluate whether the $PM_{2.5}$ mean during high-pressure blocking events had actually increased, and if so, by how much.

The Mann-Kendall test is a non-parametric statistical tool used to calculate the monotonic trend of a dataset. This test is commonly used in weather physics due to the challenges posed by many parameters and complex distributions. The test works by calculating the difference between each step in the series and the nearby steps. If the test yields a significant result, the output will be a p-value below 0.05. Kendall's τ-value is used to evaluate the monotonic increase of the dataset, where -1 indicates a total monotonic decrease, 1 indicates a total monotonic increase, and 0 indicates no trend. The τ-value can be summarized by the formula

$$\tau = \frac{C - D}{C + D},\tag{1}$$

where C is the number of concordant pairs and D is the number of discordant pairs. If the result yielded a τ-value above 0.5, the result was labelled as an clear increase. Sen's slope is a method of performing linear regression on the data. The method differs from the least squares method because it uses the median to calculate the slope. This ensures that outliers, which are common in weather data, do not affect the results. Sen's slope is calculated as

$$S_i = \frac{C_{i+1} - C_i}{t_{i+1} - t_i}, \quad \text{Sen's slope} = \text{median}(S_i)\tag{2}$$

where i represents the indices, C represents the concentration of $PM_{2.5}$, and t represents time. The program used for the Mann-Kendall test was the `pymannkendall` package in Python [9].

3.5   The measuring devices

3.5.1   The meteorological measuring devices

The wind data from both Hörby and Helsingborg used the high-performance wind sensor Vaisala WAA15A for the wind speed and Vaisala WAV15A for the wind direction. These instruments were serviced and calibrated every year or every other year, and had been in use since 1995. The WAA15A anemometer measured wind speed with an accuracy of $\pm 0.17\,\mathrm{m\,s}^{-1}$, and the WAV15A wind vane measured the wind direction with an accuracy better than $\pm 3°$ [10]. The WAA15A anemometer works by a rotating chopper disc that interrupts an infrared beam, resulting in a laser pulse proportional to the wind speed. The WAV15A wind vane uses a counterbalanced vane with an optical disc. When the vane turns, infrared LEDs detect the change in angle with the disc and phototransistors, resulting in a precise measurement of the wind angle. For rain monitoring, the Geonor T200 device had been in use for all stations since 1995. Like the wind monitor, this device had been serviced and calibrated every year or every other year. This device works by measuring precipitation with a vibrating wire sensor that detects weight changes from the water droplets[11]. The device has a measurement accuracy better than 0.1 mm. The rain measurements in Tånga was measured manually by a beaker located on a field. Thus, errors in this measurement were higher than the digital measurement devices .

The barometer that has been in use for Helsingborg is a Vaisala PTB201A for the entire period, except for the periods from April 15, 2015, to April 17, 2025, and from September 19, 2004, to May 23, 2014, when a Vaisala PTB220 was used instead. Even then, the device has been serviced every year or every other year. The PTB201A digital barometer operates using a silicon capacitive absolute pressure sensor, providing stable and accurate pressure values [12]. The sensor functions by means of a flexed diaphragm inside a capacitor that bends in response to air pressure, causing a change in the capacitor's distance and thus a variation in the current. This device measures pressure in the range of 600 hPa to 1100 hPa, with an accuracy of ± 0.3 hPa. Errors in the device may arise due to environmental factors, such as exposure to condensing gases. The Vaisala PTB220 digital barometer operates in a similar manner but offers a wider measurement range of 500 hPa to 1100 hPa, with an improved accuracy of ± 0.15 hPa [13].

- How was pressure in Ängelholm and rain in Ängelholm measured?

3.5.2   The PM2.5 mesuring devices

The measurement device used at Vavihill was the ambient particulate monitor TEOM 1400. This monitor continuously collects airborne particles less then 2.5 µg onto a filter and measures their mass using an oscillating microbalance technique [14]. The oscillating microbalance works by vibrating at a natural frequency, which changes

as particles accumulate on the filter. Since this frequency shift is proportional to the mass of the deposited particles, their total mass can be accurately determined. The precision of the monitor was $\pm 1.5\,\mu\mathrm{g\,m^{-3}}$. Thus, the monitor provides high precision and stable measurements. However, a key limitation is that it cannot distinguish between different types of particles, as it only measures total mass.

When the measuring station was moved to Hallahus, the measuring device was updated to the fine dust analysis system Palas FIDAS 200. This device works by an optical aerosol spectrometer which samples particles from an isokinetic inlet through a polychromatic light-scattering channel where the scattering angles and intensity were measured. [15]. This results in a high accuracy of $\pm 0.1\,\mu\mathrm{g\,m^{-3}}$, indicating an improvement from the other device.

The monitoring station in Malmö used several measuring devices over time, in conjunction with other equipment. Between the start of the monitoring and January 1, 2009, the TEOM 1400 monitor was used. From January 1, 2009, to December 31, 2015, the TEOM 1400, FDMS, and 8500 B or CB dryer were employed. Between January 1, 2016, and December 31, 2021, the TEOM 1405F and FDMS systems, along with the 8500 B, were in use. Finally, from January 1, 2022, the Palas FIDAS 200 monitor replaced the earlier systems. The FDMS (Filter Dynamics Measurement System) is a dynamic filter measurement system that enhances measurements by accounting for volatile and semi-volatile particles [16]. The CB dryer and 8500 B were air dryers used to prevent moisture from entering the measurement devices, ensuring accurate data by avoiding potential interference caused by water vapour.

4   Result

4.1   The evolution of PM 2.5 over time

After applying the high-pressure blocking detection method to the data from Vavihill for the entire period, a total of 298 high-pressure blocking events were identified between August 1, 1995, and October 10, 2024. Of these 298 events, 171 were removed due to insufficient PM$_{2.5}$ data, as a filter requiring 95% data coverage was applied. This left 127 relevant high-pressure blocking events. For Malmö, a total of 299 high-pressure blocking events were identified between November 20, 1995, and October 1, 2024. From these, 99 events were removed due to insufficient PM$_{2.5}$ data, again applying the 95% data coverage filter. This resulted in 200 relevant high-pressure blocking events. The result from the Mann-Kendall test can be viewed in the figures below. All of the categories had a p-value approximately equal to 0. An example plot showing the periods of high-pressure blocking events can be seen in Figure 1.
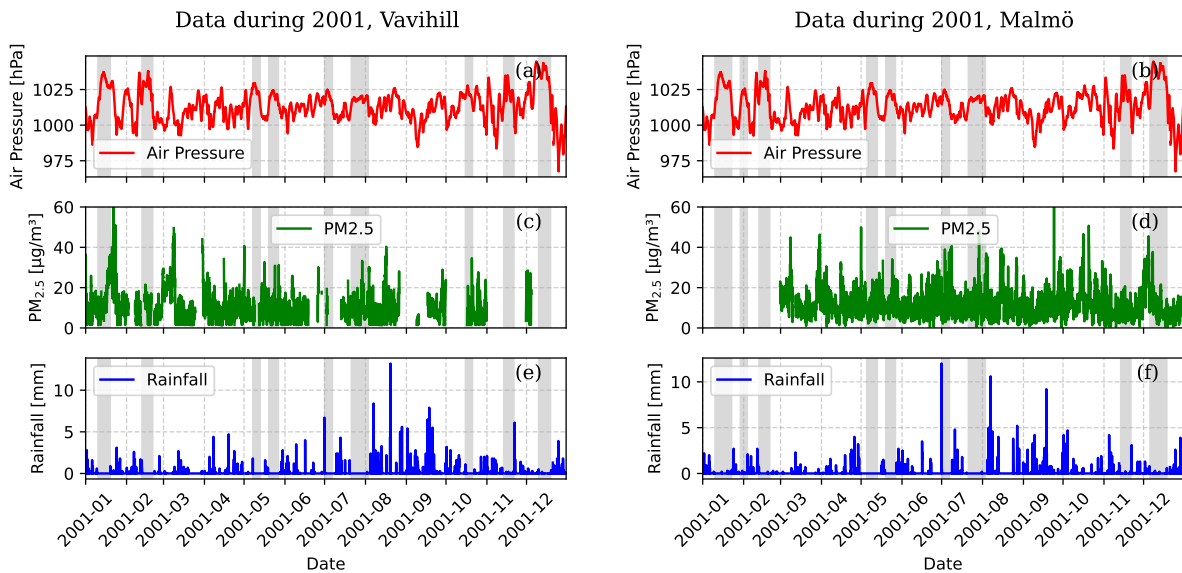

Figure 1: These example plots displays the air pressure, PM$_{2.5}$ concentrations, and rainfall during the year 2001. The periods which was indicated as periods of high-pressure blocking events are shown in gray.

The next result was to evaluate the PM$_{2.5}$ concentrations during periods of high-pressure blocking by taking the mean concentration from the start of the event. This can be seen in Figure 2. The data is compared with the PM$_{2.5}$ mean taken from periods without high-pressure blocking events. An increase in PM$_{2.5}$ concentrations can be seen in Malmö, while a slight increase can be observed in Vavihill. This is supported by the large τ-value in the case of Malmö, and slight lower in Vavihill. The Sen's slope values also indicate a stronger increase in Malmö. It is important to note that after the first five days, the number of datasets decreases, which is reflected in the increase in standard deviation.
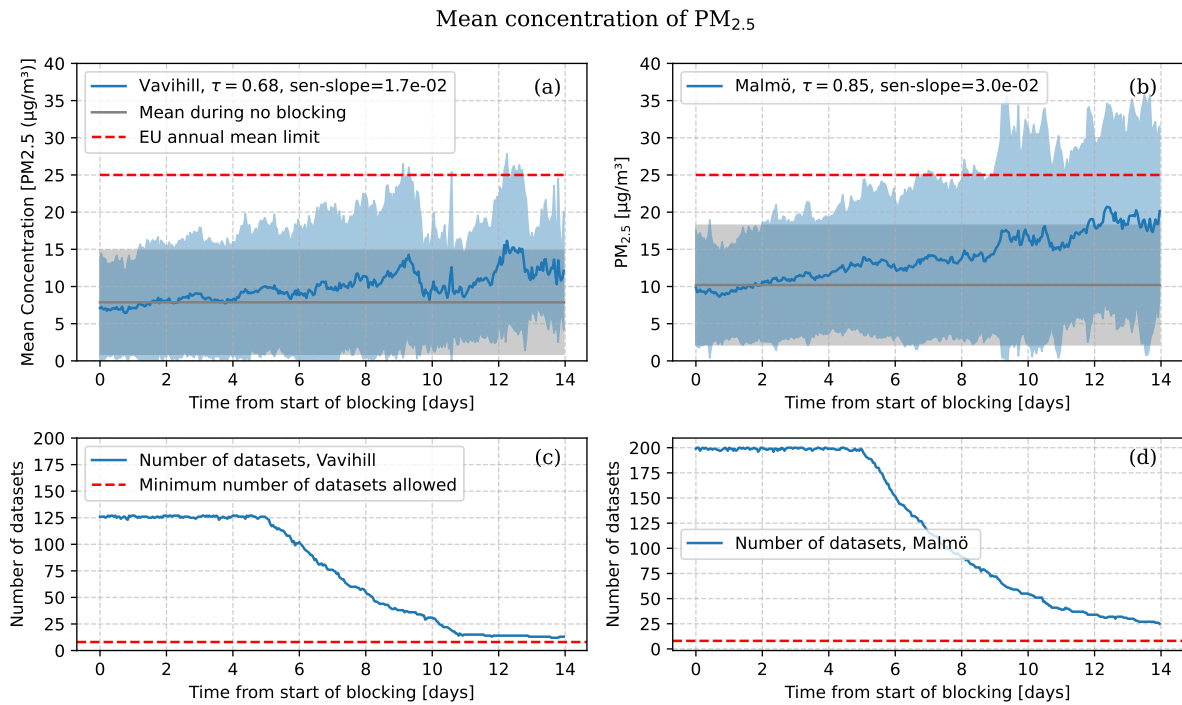
Mean concentration of PM$_{2.5}$

Figure 2: Comparison of mean PM$_{2.5}$ concentrations in Vavihill and Malmö, highlighting differences between rural and urban air quality. The shaded region indicates the standard deviation of the data.

The change in PM$_{2.5}$ concentrations in Vavihill and Malmö for different wind directions can be seen in Figure 3. One can see similarities between the wind directions for Vavihill and Malmö, although the extremes are more pronounced in Malmö. When the wind filter was applied for the Northeast direction (310° to 70°), no strong increase or high levels of PM$_{2.5}$ were detected, as supported by the τ-values being under 0.5. The same is true for the Southeast direction (70° to 190°) and almost true for the non-specific wind direction, in Vavihill. However one must note in the case of Southeast direction (70° to 190°) for Vavihill that there is a clear increase until day 9, where the levels suddenly drop. For the other directions, an increase in PM$_{2.5}$ can be seen as supported by the τ-values and Sen's slopes. Elevated levels can also be seen in Malmö for the West direction (190° to 310°), and especially in Vavihill for the SE direction (70° to 190°) where the mean concentration exceeds the EU annual mean limit.
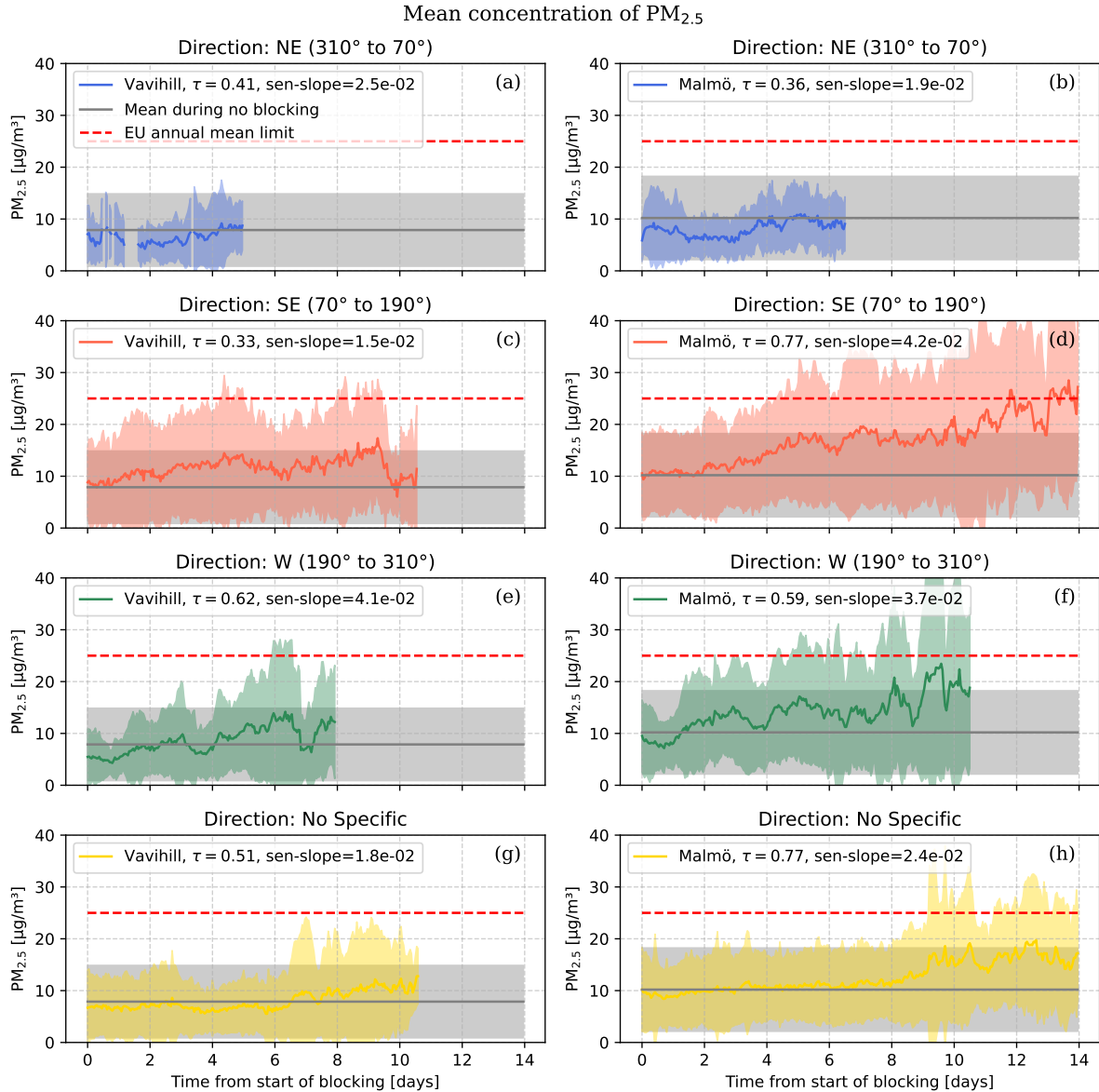
Mean concentration of PM$_{2.5}$

Figure 3: These plots show how PM$_{2.5}$ concentrations change in Vavihill and Malmö for different wind directions. In the case of Vavihill, it is important to note that 6.3% of the winds came from the Northeast (310° to 70°), 39.9% from the Southeast (70° to 190°), 21.3% from the West (190° to 310°) and 42.5% from no specific direction. In the case of Malmö, it is important to note that 7.5% of the winds came from the Northeast (310° to 70°), 24.0% from the Southeast (70° to 190°), 18.5% from the West (190° to 310°) and 50.0% from no specific direction. Note that a minimum number of datasets was still put to 8, resulting in some directions having very little data.

The seasonal change in concentrations of PM$_{2.5}$ can be seen in Figure 4. From these plots, it is clear that the concentration during the summer for both Vavihill and Malmö does not indicate an increase nor high levels of PM$_{2.5}$. A slight increase can be seen in the case of spring for both locations. A larger increase can be seen during the autumn, where high levels of PM$_{2.5}$ can be observed towards the end of the period. The winter in Vavihill indicates an increase in the PM$_{2.5}$ concentrations, although the standard deviation indicates highly dispersed data. Although the τ-value during the winter in Malmö is relatively low, Sen's slope indicate a stronger increase. From the graph one can see an increase in PM$_{2.5}$ concentrations, although the levels seem to lower towards the end of
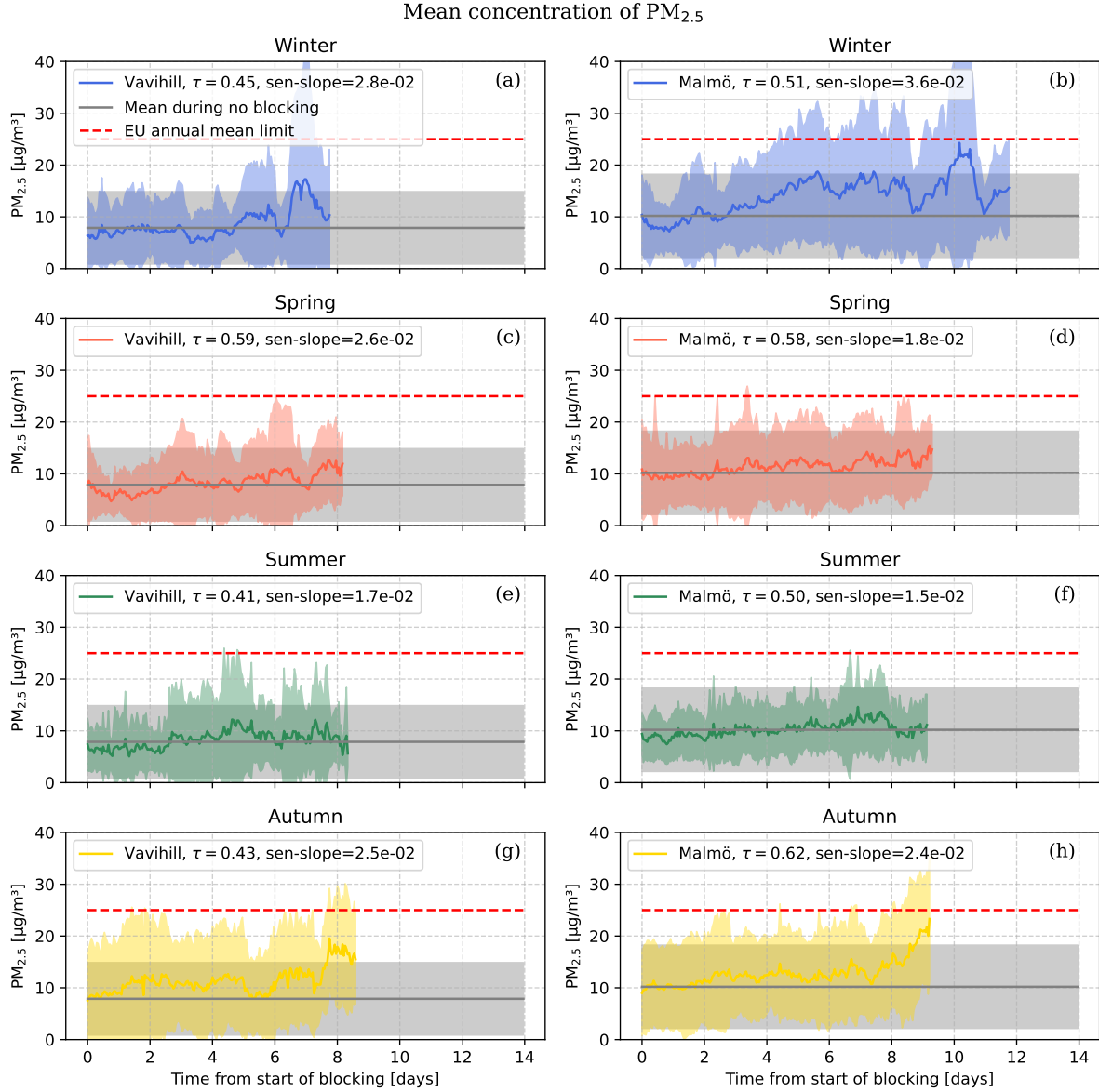
the period.

Figure 4: These plots show how PM$_{2.5}$ concentrations change in Vavihill and Malmö for different seasons. It is important to note that 21.1% of the blocking events occurred during the winter, 27.4% during the spring, 24.2% during the summer and 27.4% during the autumn. In the case of Malmö, It is important to note that 24.0% of the blocking events occurred during the winter, 34.0% during the spring, 18.0% during the summer and 24.0% during the autumn. Note that a minimum number of datasets was still put to 8.

The increase in PM$_{2.5}$ concentrations depending on the strength of the high-pressure blocking event can be seen in Figure 5. From the plots, we can observe similar behaviour in the two locations. In the case of weaker high-pressure blocking events no clear monotonic increase nor highly elevated levels of Pm$_{2.5}$ can be seen. In the case of medium strong high-pressure blocking events we see a stronger increase in the case of Vavihill and weaker in Malmö from the τ-value and Sen's slope value. However when observing both plots one can see an increase for both plots around day 9. In the case of stronger high-pressure blocking events we see a strong increase in the case

for Malmö, and not as clear increase in the case of Vavihill. However when viewing the plots one can observe that the levels of $PM_{2.5}$ in the case of Vavihill exeed the normal range towards the end of the period. In the case of Malmö we can see a very strong increase towards the ned, where we reach the EU annal mean limit.
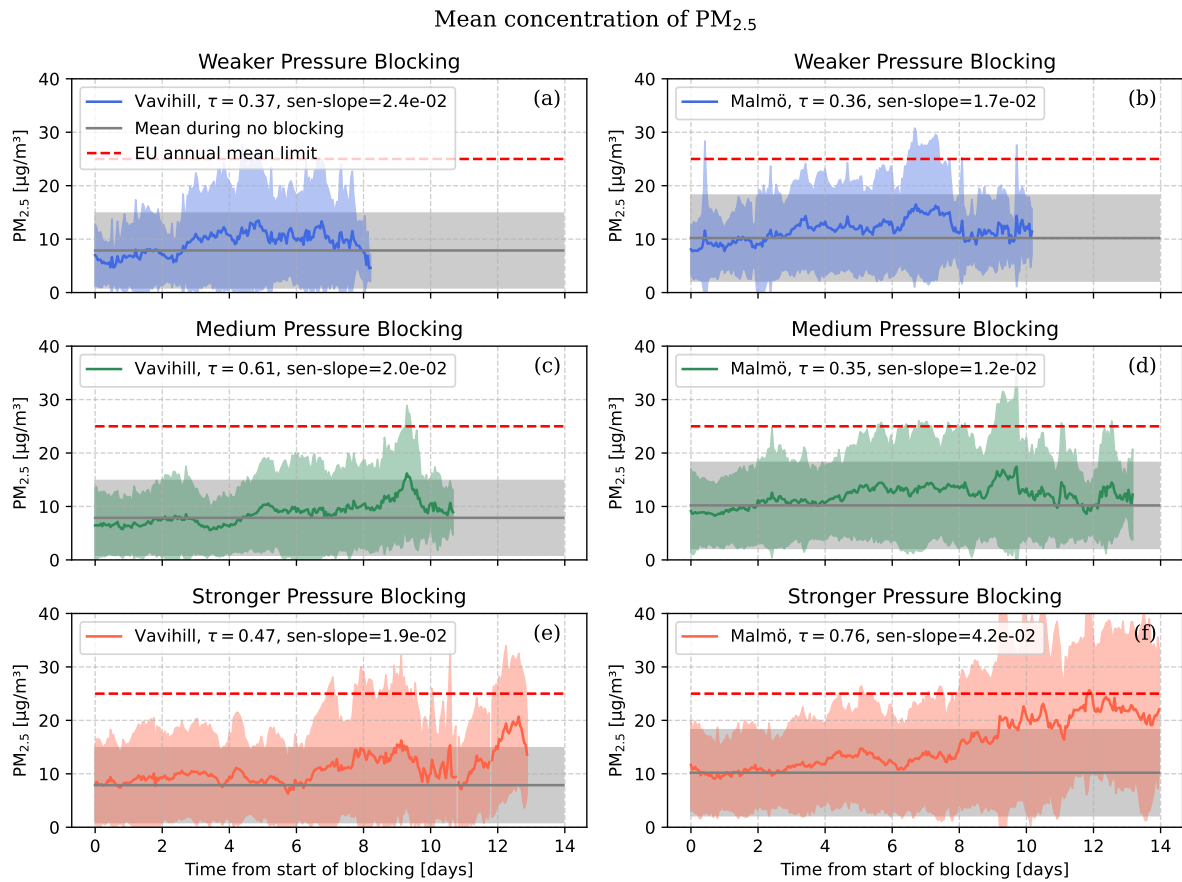

Figure 5: These plots show how $PM_{2.5}$ concentrations change in Vavihill and Malmö for different pressure strengths for high-pressure blocking events. In the case of Vavihill, It is important to note that 20.5% of the blocking events occurred with a mean pressure below 1020 hPa 44.9% occurred between 1020 and 1025 hPa and 34.6% occurred with a mean pressure over 1025hPa. In the cas of Malmö, it is important to note that 17.0% of the blocking events occurred with a mean pressure below 1020 hPa 48.5% occurred between 1020 and 1025 hPa and 34.5% occurred with a mean pressure over 1025hPa. Note that a minimum number of datasets was even here put to 8.

4.2 The frequency of high pressure blocking events

The last task was to determine whether high-pressure blocking events have become more common. When looking at the number of high-pressure blocking events per year, no significant change in frequency could be seen (see Figure 6). Since the highest levels of $PM_{2.5}$ occurred toward the end of the events (see Figure 2, Figure 3, Figure 4, and Figure 5), the frequency of longer high-pressure blocking events was also examined. However, no increase could be observed in any of the cases. More interestingly a small decrease can be observed from the τ-values and the Sen's slope values. However one must note that the p-values are much larger here than before, indicating towards a more random system.
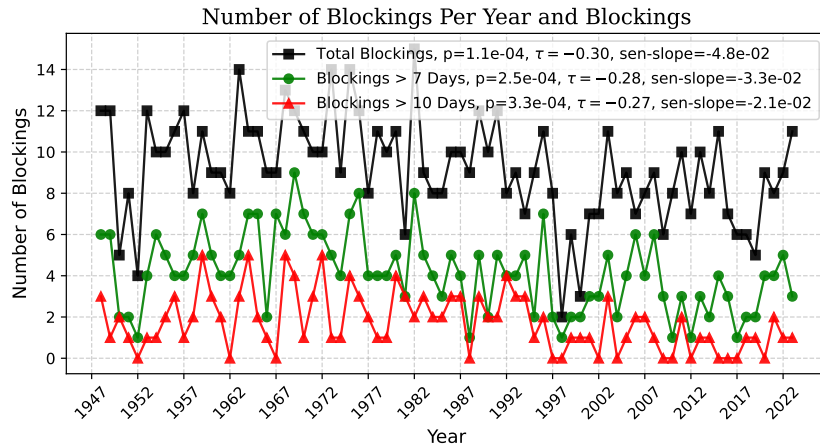
Figure 6: fig: This plots shows the change in frequency of high-pressure blocking events. The plots also indicates the change in events longer than 7 and 10 days.

In Figure 7, the number of days under high-pressure blocking events per year can be seen. Here, the total, seasonal, and pressure strength dependence can be observed. The reason for not including the directional dependence is that this was not available from the data. However, these plots show no increase in the number of days under high-pressure blocking events. Even here a slight increase can be seen in most plots, especially the total blocking days per year (h).
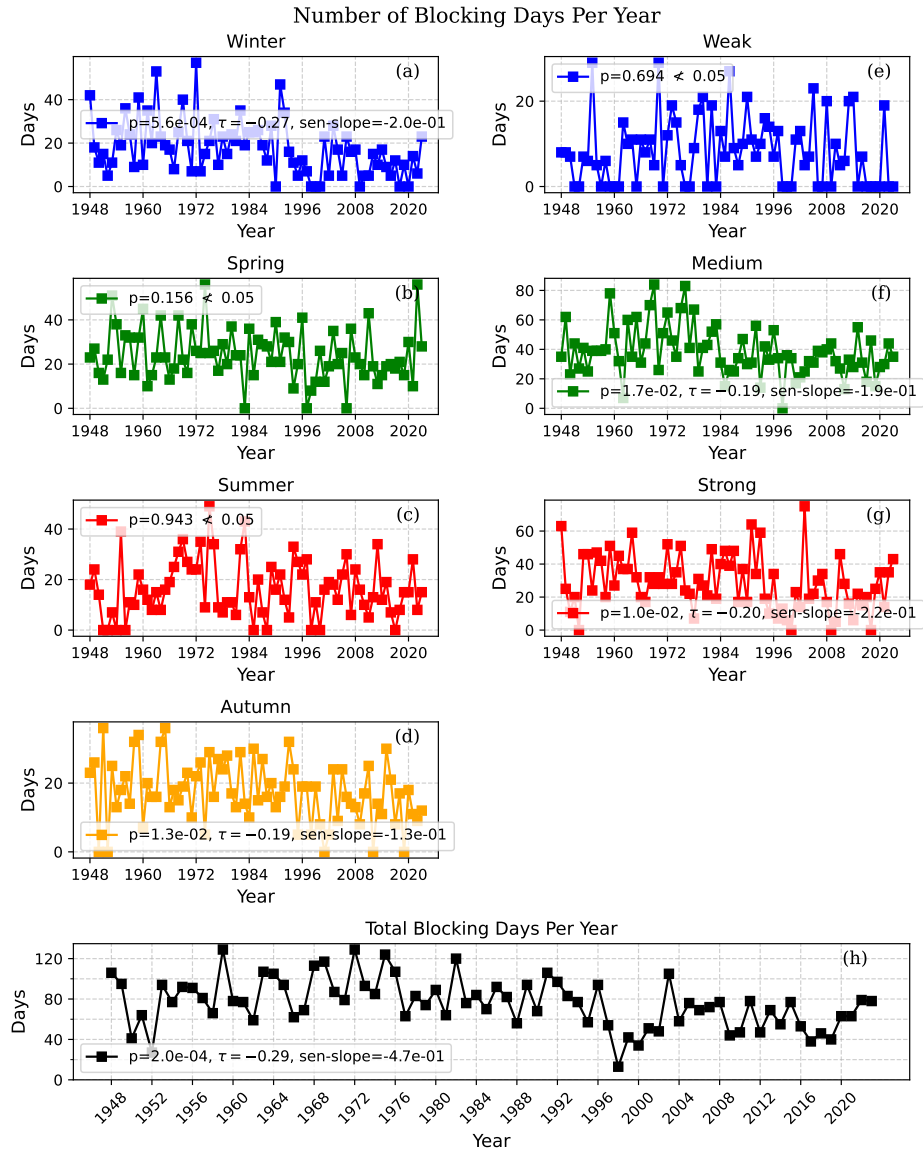
Figure 7: These plots show the change in frequency of days under high-pressure blocking events. The number of days under a high-pressure blocking event each year, during each season, and for different pressure strengths can also be seen.

5   Conclusion

6   Outlook

References

[1] NASA. Haze over Europe. https://earthobservatory.nasa.gov/images/11219/haze-over-europe, March 2003.

[2] John F. B. Mitchell, Jason Lowe, Richard A. Wood, and Michael Vellinga. Extreme events due to human-induced climate change. *Philosophical Transactions of the Royal Society A: Mathematical, Physical and Engineering Sciences*, 364(1845):2117–2133, 2006.

[3] Anthony R. Lupo. Atmospheric blocking events: A review. https://nyaspubs.onlinelibrary.wiley.com/doi/abs/10.1111/nyas.1455, December 2020.

[4] Wenyue Cai, Xiangde Xu, Xinghong Cheng, Fengying Wei, Xinfa Qiu, and Wenhui Zhu. Impact of "blocking" structure in the troposphere on the wintertime persistent heavy air pollution in northern China. *Science of The Total Environment*, 741:140325, 2020.

[5] Vlado Spiridonov and Ćurić Mladjen. Cyclones and Anticyclones | SpringerLink. https://link.springer.com/chapter/10.1007/978-3-030-52655-9_17, November 2020.

[6] Judit Bartholy, Rita Pongracz, and Margit Pattantyús-Ábrahám. European Cyclone Track Analysis Based on ECMWF ERA-40 Data Sets. *International Journal of Climatology*, 26(11):1517–1527, 2006.

[7] Noelia Otero, Oscar E. Jurado, Tim Butler, and Henning W. Rust. The impact of atmospheric blocking on the compounding effect of ozone pollution and temperature: A copula-based approach. *Atmospheric Chemistry and Physics*, 22(3):1905–1919, 2022.

[8] European Environment Agency. Europe's air quality status 2024. https://www.eea.europa.eu/publications/europes-air-quality-status-2024, 2024.

[9] Hussain, Md. and Mahmud, Ishtiak. pyMannKendall: A python package for non parametric Mann Kendall family of trend tests. *Journal of Open Source Software*, 4(3):1556, July 2019.

[10] VAISALA. Wind Set WA15 and WA25. https://www.vaisala.com/en/products/weather-environmental-sensors/wind-set-wa15, January 2021.

[11] GEONOR, Inc. T-200B Series All Weather Gauge. https://www.geonor.com/t-200b-all-weather-precipitation—rain-gauge, 2019.

[12] VAISALA. PTB 200 DIGITAL BAROMETERS USER'S GUIDE, February 1993.

[13] VAISALA. PTB220 Series Digital Barometers USER'S GUIDE, August 2001.

[14] Thermo Fisher Scientific Inc. TEOM® Series 1400a Ambient Particulate (PM-10) Monitor Operating Manual, 2007.

[15] PALAS GmbH. Operating Manual: Fidas® Fine Dust Monitor System.

[16] Thermo Scientific. 8500 FDMS Filter Dynamics Measurement System, 2010.